Assessing Damage, Sorptivity, Air Content, and Strength of Portland Cement Concrete Pavements in Indiana

Zhifu Yang[1], Jason Weiss[2], Jan Olek[3], and Tommy Nantung[4]

Abstract

A field condition assessment was performed for selected portland cement concrete pavements (PCCP) in the state of Indiana. Five pavement sections (including a 25 year old un-trafficed section) were selected based on age, traffic, and overall performance. After a field survey and site inspection, cores were taken from these pavements and used for laboratory analysis. The cores were visually inspected, after which they were sectioned and used for air void analysis, microscopic investigation of cracking, water absorption, and splitting tensile strength. Large irregular air voids were observed in each pavement core. The hardened concrete air content was observed to vary both between the different pavement sections and between the top and bottom layers of the pavement. In addition, the hardened air content in the pavements was found to vary from 4 to 13% by volume. Micro-cracks were observed in some pavements that appeared at the aggregate paste interface, through weak aggregates, and around air voids. In damaged pavements, the sorptivity of the top layer of the pavement was higher than that of the middle or bottom layer. The magnitude of variation in sorptivity appears to be related to the age and performance of the pavement. This is in agreement with the results from laboratory-cured specimens, in which freeze and thaw damage influences both the short-term and long-term sorptivity of concrete.

Keywords: Concrete pavements, Condition assessment, Water absorption, Cracking, Air content, Strength

[1] Zhifu Yang, Assistant Professor, Concrete Industrial Management, Department of Engineering Technology and Industrial Studies, Middle Tennessee State University, Box #19, Murfreesboro, TN 37132

[2] Jason Weiss, Associate Professor, School of Civil Engineering, Purdue University, 550 Stadium Mall Drive, West Lafayette, IN 47907-2051

[3] Jan Olek, Professor, School of Civil Engineering, Purdue University, 550 Stadium Mall Drive, West Lafayette, IN 47907-2051

[4] Tommy Nantung, Section Manager, Research Division, Indiana Department of Transportation, 1205 Montgomery Street, West Lafayette, IN 47906

Introduction and Background

Portland cement concrete pavements (PCCP) undergo drying and wetting, thermal cycling, and traffic loading when they are in service. As a result, micro-cracking may occur that will either remain as distributed microcracks throughout the pavement or coalesce to form larger cracks which eventually manifest themselves as visible cracks. It is the hypothesis of this work that these micro-cracks may enable more rapid transport and ingress of water and aggressive agents, thereby reducing the life-cycle performance of PCCP.

Several studies have investigated the role of microcracking in concrete performance. Wiens et al. (1997) observed that fine, distributed micro-cracks permitted water to penetrate into high strength concrete resulting in significant weight changes during freezing and thawing. Similarly, Fagerlund (1997a) reported that during repeated freeze and thaw cycling micro-cracking developed that accelerated water absorption, thereby accelerating freeze and thaw damage. Zhou et al. (1994) reported that preloading resulted in the premature failure of specimens that were exposed to freezing and thawing. Wang et al. (1997) showed that cracks, even smaller than 200 microns, can alter the permeability of hardened concrete by several orders of magnitude. In studies on reinforced concrete elements Yoon et al. (2000) illustrated that cracks caused by loading can accelerate salt ingress leading to more rapid corrosion rates. Similarly, Qi et al. (2003) illustrated that plastic cracking also accelerates the corrosion of reinforcing steel. Based on these findings, it is clear that cracking and localized damage may have a significant impact on reducing the long-term durability of concrete pavements and structures.

Recently, life-cycle performance models have been proposed as a method to predict how concrete facilities will perform (Hoerner and Darter 1999, Fagerlund 1997b, and Bentz et. al. 2001). These models are frequently based on either empirical evidence or theoretical models that consider the properties of concrete to be those of a well-cured, undamaged specimen. However, the impact of cracking on transport properties and durability of concrete is important, and models that only consider the properties of well-cured undamaged specimens may provide misleading, unconservative, and overly optimistic results that may not truly represent the behavior of field concrete. Research is needed to better understand how cracks influence the long-term performance of concrete pavements and structures. It is essential for the development of future life-cycle models that the damage that exists in concrete pavements in service is known.

Research Significance

This study has investigated the mechanical and transport properties of cores extracted from portland cement concrete pavements (PCCP) of different ages that have exhibited different levels of wear and damage. The objective of this work was to identify the performance related characteristics of typical paving mixtures in Indiana and to describe the extent of damage that exists in field concrete. It is expected that this work will be eventually used in the development of life-cycle models that consider physical damage. Specifically, this work is useful for quantifying the damage that exists in real pavements and developing the link between cracking and increased water absorption for use in performance models.

Pavement Survey

Four different sites located in the state of Indiana were selected for this investigation. The sites were selected to represent pavements that were showing signs of premature deterioration as well as older pavements that were providing reasonable performance. To determine which sites would be used, information was obtained from maintenance engineers, pavement condition reports from the Indiana Department of Transportation (INDOT), and the visual examination of PCC pavements.

Table 1 provides details of the location, age, thickness, traffic level, and quality index of the pavements from which cores used in this study were obtained. The first site (I-465) represented a newly constructed pavement that had not been opened to traffic to provide a baseline of the typical concrete properties that could be expected from a newly constructed concrete pavement before the section experiences any weathering or exposure to traffic. The second site (I-70) that was chosen was a relatively young (approximately 6 years old) pavement that had shown signs of premature deterioration and been rated poorly (i.e., Pavement Quality Index (PQI) is less than 64 by the Indiana Department of Transportation (INDOT) (Pavement Management Unit, INDOT 2000)). The third site (I-469) consisted of a middle-aged pavement (14 years old) that had exhibited a low PQI and premature deterioration mainly in the form of faulting and cracking. The final site (I-65) was an older pavement (25 years old). The I-65 site was particularly well suited for this investigation since it provided a section that was trafficed (I-65-T) as well as a section that was constructed at the same time but that had remained essentially untrafficed (I-65-U), thus enabling the effects of traffic to be separated from environmental effects. It can be seen that the pavements investigated represent a wide range of traffic levels, ages, and performance.

Coring of Pavement Sections

After arriving at each site, traffic was diverted from the section of the pavement that was investigated and a visual examination of the site was performed. Based on the visual inspection, a typical slab was selected for core sampling. Five cores were taken from each slab using an approach that was similar to that used by Van Dam et al. (2001). Two different size cores were taken (a 102 mm (4 in) diameter and a 152 mm (6 in) diameter), depending on the location of the core in the slab. The smaller cores were typically preferred at the joints to minimize the potential for intersecting a dowel bar. Figure 1 illustrates the coring locations in a typical slab and shoulder. This coring pattern was followed for all but one (newly constructed I-465) pavement sections. Since I-465 section was never exposed to traffic, the exact location of the cores is insignificant and therefore was not recorded. In general, one core was taken from the center of the slab in the wheel path (W1), one core was taken from the wheel path near the joint (WJ2), one core was taken from the center of the slab (C3), one core was taken from the center of the shoulder (S4), and the last core was taken from the corner near the joint (CJ5). It is assumed that the wheel path and the center of the slab are exposed to both environmental attack and traffic loading, while the shoulder is primarily subjected to environmental exposure. By comparing these locations, the impact of traffic loading, joint and edge effects and environmental exposure can be assessed. After the cores were extracted, they were taken back to the laboratory for further analysis as described in the following section.

Table1. Pavement Sections Selected for Sampling and the Related Information

Pavement	Age (Year)	Thickness mm (in.)	Traffic Level		PQI[2]	Location
			AADT[1]	%Truck		
I-465	0	356 (14.0)	None	None	–	Indianapolis, Indiana
I-70	6	363 (14.3)	96,000	10%	64	Senate Ave to 7.7 MI E of I-465 @ East St., Indianapolis
I-469	14	295 (11.6)	19,000	4%	61	I-69 to 0.7 MI W of SR 1, Fort Wayne
I-65-U	25	315 (12.4)	None	None	–	Intersection of I-65 and I-70 near North Split, Indianapolis
I-65-T	25	315 (12.4)	140,000	7%	66	Intersection of I-65 and I-70 near North Split, Indianapolis

1 AADT- Annual Average Daily Traffic
2 PQI – Pavement Quality Index (Pavement Management Unit, INDOT 2000), it is a composite index to indicate the surface quality of pavement with a 100 point scale: excellent (100-90), good (90-80), fair (80-70), and poor (<70). It correlates with International Roughness Index (IRI), Pavement Condition Rating (PCR), and Rutting (Rut).

Laboratory Analysis of Field Cores

After the cores were delivered to the laboratory, they were visually inspected and any visible damage was recorded. The core samples were then tested using ultrasonic pulse velocity to inspect for any significant internal flaws. After the non-destructive testing was completed, the cores were sectioned by cutting alternate two 13 mm (0.5 inch) thick discs and one 51 mm (2 inch) thick disc as illustrated in Figure 2. The core sections were then used for microscopic evaluation, air void determination, water absorption measurement, and splitting tensile strength determination. The following sections describe how the specimens were prepared for each of these test procedures.

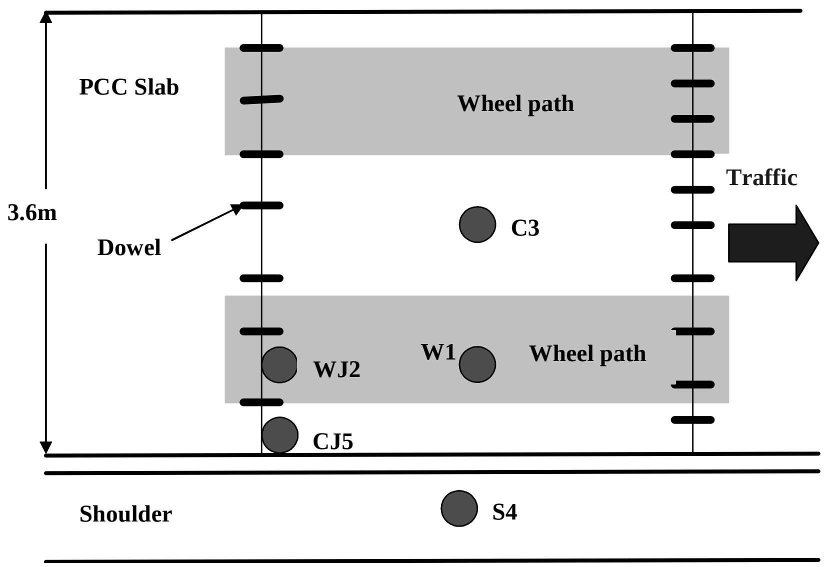

Figure 1. Illustration of coring locations from a typical slab

Note: Core W1- Sample No. 1, taken from the center of the wheel path; Core WJ2- Sample No. 2, taken across the joint and between dowels of the wheel path; Core C3- Sample No.3, taken from the center of the slab; Core S4- Sample No. 4, taken from the shoulder; Core CJ5- Sample No. 5, taken from the corner and joint of the slab edge

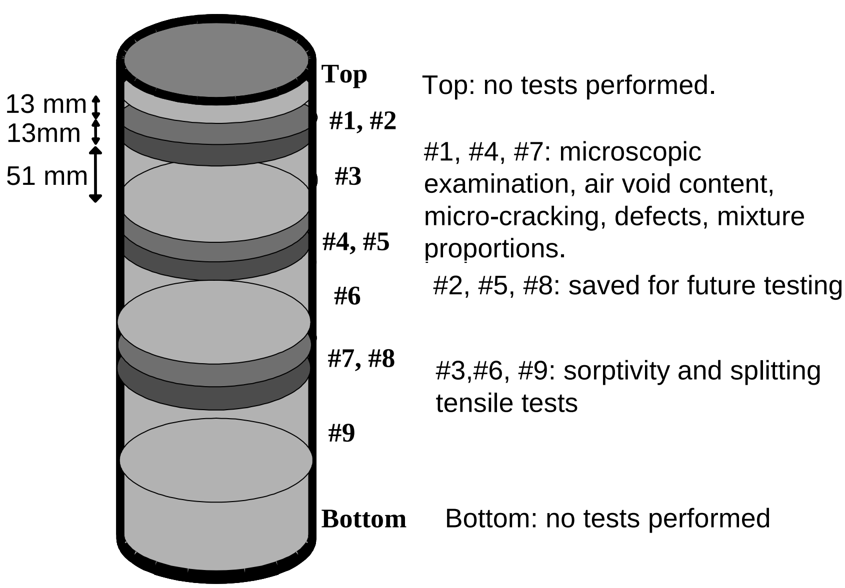

Figure 2. Illustration of sectioning a typical core for laboratory investigation

Visual Inspection. The cores were first visually inspected to determine whether any visible damage, segregation, or construction defects could be observed. Any damage that was observed was noted and recorded.

***Ultrasonic Pulse Velocity (UPV) Testing*.** Ultrasonic Pulse Velocity (UPV) test (ASTM C597 1997) was used to evaluate the internal damage, uniformity, and relative quality of concrete. In these tests, two transducers were used to measure the time it took to transmit an ultrasonic wave across the diameter of the specimen. The wave speed was calculated by dividing the distance between the transducers (nominally 152 mm or 100 mm) by the time that it took for the wave to cross the specimen. The longer the wave transmission time (i.e., the slower the wave speed) the more internal damage could be expected in the core. A V-meter (manufactured by James Instrument) was connected to a pair of 54 kHz transducers that were coupled to the opposite sides of the core using petroleum jelly. One transducer was used as the pulser while the other was used as the receiver and the time that it took the wave to transmit across the cylinder (in milli-seconds) was recorded. The UPV was measured in two perpendicular directions every 51 mm from the top of the core to bottom of the core since the cracks that form may have a specific orientation. The average wave speed that was measured in the two directions was reported.

Microscopic Examination. After the UPV measurements, the cores were sectioned into smaller disks as shown in Figure 2. The 13 mm disks were selected for microscopic evaluation. One surface of the disks was polished using a bench-top lapping wheel. Water was used as a lubricant and a siliconcarbide (SiC) abrasive was applied with sizes ranging from No. 100 to No. 600. The final polishing was performed on a glass plate using No. 800 and No. 1000 SiC abrasives. The samples were then placed on a Roiswal traveling table and the volumetric percentages of aggregates, paste, and air voids were determined based on the modified point count method (ASTM C457 1998). An optical microscope set at a magnification of 100X was used to examine the polished slices to assess the general condition and crack patterns of the concrete. Typical damage patterns were recorded using an image acquisition system.

Water Absorption and Sorptivity Determination. Water absorption tests are being increasingly used to evaluate concrete durability in aggressive environments (Lockington et al. 1999 and Wilson et al. 1999). In this study, the 51 mm (2 in) disks that were sectioned from either 152 mm (6 in) or 102 mm (4 in) diameter concrete cores were used to determine the water absorption properties of the concrete and the rate at which this water was absorbed. The disks were first air dried and their circumference was sealed with an epoxy to ensure that moisture exchange will only take place through the top and bottom faces of the disks. All the disks were then pre-conditioned in an environmental room with a controlled temperature of 23 °C and relative humidity of 50% for 14 days to enable the specimen to reach a relatively uniform state of moisture. A ponding dyke was placed on the top of the disks and the bottom was covered with plastic wrap to prevent moisture loss. Water was added to the inside of the dyke until it reached a depth of approximately 15 mm. Periodically (at 0, 0.1, 0.2, 0.5, 1, 5, 12, 24, 48, 96 hours, then at 96 hour intervals after that) water was removed from the surface of the disks, the surface was toweled dry (to achieve saturated surface dry conditions), and the mass of the specimen was recorded. After the mass was recorded, water was immediately reintroduced to the top of the specimen and remained on the surface until the next measurement was performed. This testing procedure was used to define the total amount of water that has been absorbed in the concrete as well as the rate of absorption (sorptivity) as described later in this paper.

In addition, experiments were conducted using laboratory-cured specimens to evaluate how damage influences the short-term sorptivity of concrete and how damage and air content influence the long-term sorptivity of concrete. Concrete prisms (76 ×102 ×406 mm) were prepared using a concrete with compositions similar to that used for concrete pavements in Indiana (cement: crushed limestone: natural river sand: water by mass = 1:2.85:2.37:0.42). The concrete was cast into the steel molds, compacted on a vibrating table, and stored in a moist and sealed environment for 24 hours. The specimens were then demolded and cured in a moist room (greater than 98% relative humidity) for 13 months. After curing, each concrete prism was cut into two small prisms (76 ×102 ×202 mm). These prisms were dried in an oven at 50°C for 3 weeks and then saturated with water under vacuum treatment. After vacuum saturation, all the specimens were adjusted to individual degrees of saturation by drying them in air at 23°C and 50% relative humidity for different times typically from 2 hours to 3 days. After a desirable degree of saturation was reached, the specimen was exposed to freezing and thawing with one cycle per day to induce damage. Resonant frequency was used to monitor the damage development during freezing and thawing. The relative dynamic modulus (E/E_0) was calculated following ASTM E1870 and used as a damage index to indicate different freeze and thaw damage levels. After a desirable freeze and thaw damage was induced, the specimen was cut into 76 ×102 ×51 mm slices and then dried in an oven at 50°C for 2 weeks. After drying, all the concrete slices were used for sorptivity test following the procedures described previously. Detailed information on the materials properties, mixture proportions, vacuum saturation, and freeze and thaw testing was described in Yang (2004).

Strength Evaluation. After the water absorption tests were completed, splitting tensile tests were performed on the 51 mm (2 in) sections of the core following the approach outlined in ASTM C 496 (1996) with a loading rate of 0.69 MPa/min (100 psi/min). For each core, a total of three specimens were tested. These specimens were collected at an average depth of 38 mm (1.5 inches), 114 mm (4.5 inches), and 191 mm (7.5 inches).

Experimental Results and Discussions

Visual Inspection. No visible cracking or segregation was observed in the majority of the cored cylinders. It should however be noted that one specimen taken from I-65-U section was partially cracked. In addition, as shown in Figure 3, evidence of construction defects in the form of irregular voids up to 25 mm (1 in) in diameter were observed at the depth about 127 mm (5 inches) below the top surface in the I-465 pavement. These voids appear to be remnants of an unfilled vibrator trail. Further discussion of the I-65 and I-465 cores is provided in microscopic investigation section of this paper.

Ultrasonic Pulse Velocity (UPV). Figure 4a shows the result of UPV measurements for cores from each site as a function of pavement depth (distance from pavement surface). The average UPV value of the five locations of the selected slab from each site was used. However, the cracked core from I-65-U section was not included in calculating the average. It can be seen that the UPV values range from 4600 m/s to 4900 m/s (251 ft/min to 268 ft/min) for the uncracked cores which is consistent with what would be expected in these concretes. Figure 4b shows a comparison of UPV measurements for cracked and uncracked cores from I-65-U. It can be seen that the presence of visible cracks resulted in a dramatic reduction in the wave speed.

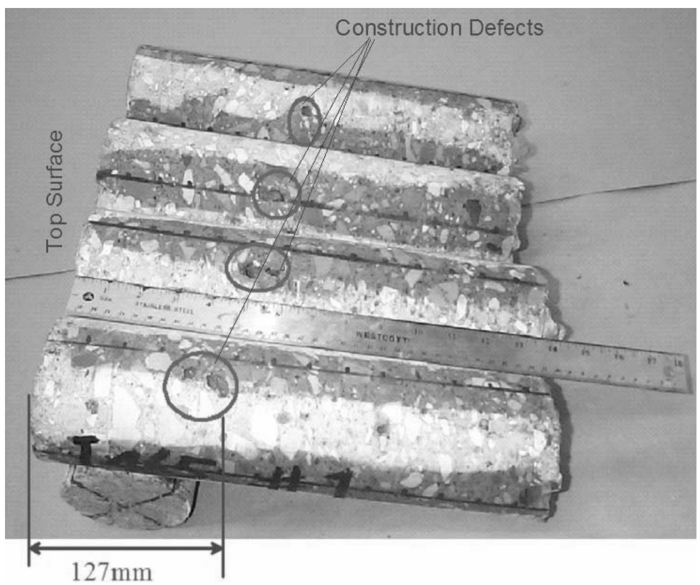

Figure 3. Photograph showing construction defects below surface of an I-465 pavement section

At this time it should be noted that many factors may affect the UPV measurements, including specimen dimension and geometry, properties of constituent materials, and degree of saturation. However, only large internal flaw or significant changes in uniformity will have noticeable influence on UPV (Suaris and Fernando 1987 and Popovics et al. 1990). Air voids, especially entrapped air, and presence of microcracks may reduce the UPV somewhat, but not significantly. This can be further confirmed by comparing Figures 4a and 4b. While some changes in the average values of UPV were observed for cores with no visible cracks (Figure 4a), mostly reflecting variability in age, air contents and microcracks, the truly significant drop in UPV was associated with the presence of visible cracks. This indicates that UPV techniques may be useful for locating the cracks in PCC pavements, however the size of the flaw that can be detected must be sufficiently large (i.e., of the size that it would approach being visible cracking).

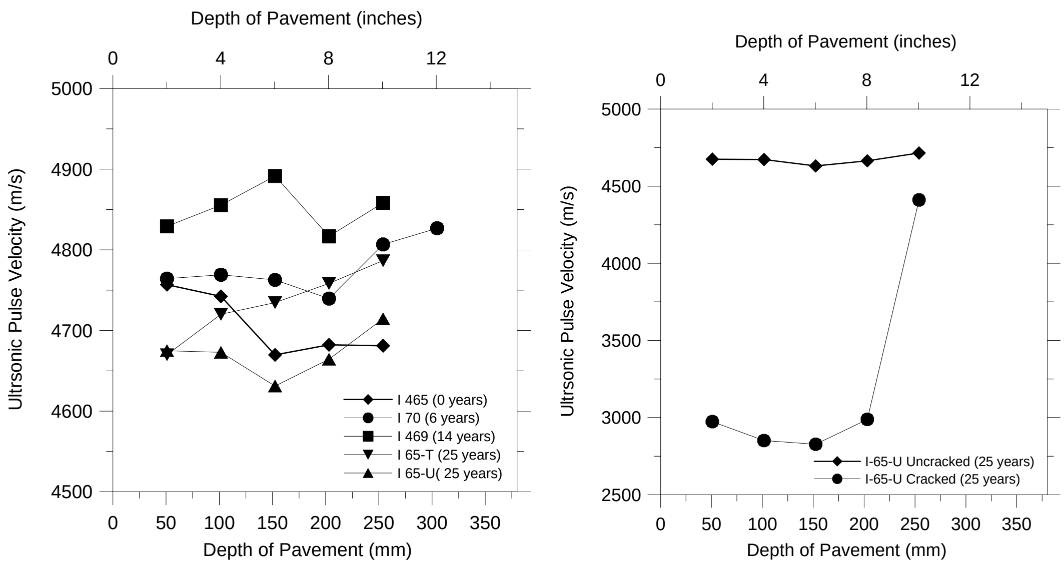

(a) (b)

Figure 4. Variation of ultrasonic pulse velocity with pavement depth, (a) average of five cores for all pavement sections, and (b) two cores from I-65-U

Microscopic Examination. The parameters associated with the air void system evaluated during the microscopic examination of the specimens included the volumetric percentage of air voids, specific surface area, and spacing factor. In addition, the paste and aggregate content were also determined.

The air void contents were found to vary from top to bottom of each pavement, and from one pavement to another. Figure 5a illustrates the variation in hardened air content as a function of pavement depth for the two cores from the newly constructed pavement section of I-465. It can be seen that the air contents vary from 4.9% to 13.1% with an average total air content of 9.8%. Very high air content was observed near the mid-depth of the pavement due to the presence of very large irregular entrapped-air voids ranging from 2.5 mm (0.1 inches) to 17 mm (0.7 inches) in diameter which may suggest that insufficient vibration occurred in this pavement. On the contrary, low air content near the top surface was observed (4.9 %), which may be attributed to the over-vibration of some portions of the surface during construction. Paste and aggregate contents were also estimated for the same two cores. The volume of paste was found to be in the range from 18.9% to 23.8% and the volume of aggregate was in the range from 65.4% to 72.8%. It should also be noted that the distribution of the paste and aggregate fractions were relatively uniform throughout the depth of the pavement.

Figure 5b shows a comparison of the overall trend in the average value of air content for all the pavement sections investigated in this research. The air contents of three pavement sections (I-65-T, I-465, and I-65-U) are all relatively high. The sections from I-469 and I-70 appeared to have relatively typical air contents (5.0% to 7.6%). Concrete with an appropriate air void size and distribution can resist the freezing and thawing damage. Table 2 separates entrained air from entrapped air based on the size and shape of the air void using microscopic examination. It can be seen that the entrained air content varies from 3.4% to 7.3% in the pavement sections investigated. As the air content increases, the freeze-thaw resistance is typically thought to improve, however a reduction in strength is typically observed. Concrete with unevenly distributed air or large volumes of entrapped air may be susceptible to freezing and thawing attack. However, other than the sections that appeared to be over vibrated (I 465), the air void spacing was uniform and consistent with acceptable spacing (ASTM STP169C 1999).

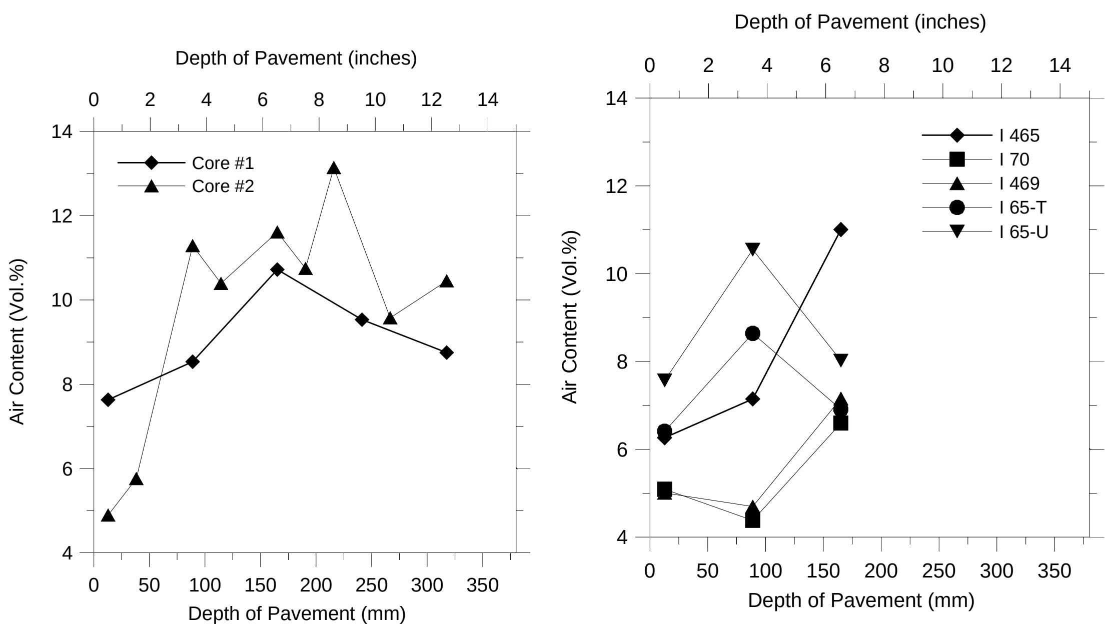

(a) (b)

Figure 5. Variation in total hardened air contents in pavements, (a) two cores (#1 and #2) from I-465 section, and (b) average of five cores from five pavement sections

Typical cracking patterns showed cracks that developed at the interface between the aggregate and the paste, in the paste, or through the weak aggregates. Figure 6a shows examples of the cracked aggregate and paste. It can be seen that crack propagated through both the fine aggregate and the paste implying that cracking occurred at later age, and was possibly induced by traffic or environmental attacks such as freeze and thaw cycles. Figure 6b provides an illustration of paste cracking, in which cracks extended to the void. Figure 6c illustrates interface cracking. This type of cracking is typically associated with damage that occurs due to loading as a result of dissimilar strains that develop between the aggregate phase and the paste phase.

Table 2. Parameters of Air Void System

Pavement Section	Air Void System				
	Average Air Content (vol. %)			Specific Surface Area *	Spacing Factor
	Total	Entrained	Entrapped	mm^2/mm^3 ($in.^2/in.^3$)	mm (in.)
I-65-T	9.6	7.3	2.3	12.3 (313.1)	0.267 (0.0105)
I-469	7.3	4.1	3.2	9.5 (240.3)	0.356 (0.014)
I-70	4.6	3.4	1.2	14.5 (369.4)	0.330 (0.013)
I-465	11.5	7	4.5	8.3 (209.6)	0.244 (0.0096)
I-65-U	9.3	6	3.3	10.2 (258.7)	0.356 (0.014)

* *Specific surface area was calculated based on the total air content (entrapped and entrained)*

Water Absorption and Sorptivity. A typical plot of the change in mass of the samples due to water absorption per unit area of the surface that was exposed to water was plotted as a function of the square root of time and is shown in Figure 7. It can be seen that this graph contains four main regions: 1) the region of short-term water absorption, 2) transition region, 3) the region of long-term water absorption, and 4) the total absorption at a specific time (368 hours). The slopes of the curve in region 1 and 3 describe the rate of cumulative water absorption per unit area at short and long terms respectively. This water absorption was fitted using linear regression and the equation obtained was used to describe capillary actions at both short and long terms (Bentz et al. 2001).

In this paper the short-term rate of water absorption (i.e., initial sorptivity or short-term sorptivity) was determined based on the initial seven hour water absorption. It is thought to be a measure of how quickly the water fills capillary pores (Marchand et al. 1997 and Martys and Ferraris 1997) and cracks. It is dependent on the preconditioning (initial water content and drying) and pore size and distribution of concrete. Cracks may permit an increase in water ingress. As a result, concretes with higher degree of deterioration tend to have higher short-term sorptivity values. Figure 8 shows the results of how freeze and thaw deterioration influences the short-term sorptivity of concrete using laboratory-cured specimens in this study. It can be seen that the short-term sorptivity increases with a decrease in the relative dynamic modulus (or an increases in the freeze and thaw damage). However, two slopes were observed with a knee point occurring when the relative dynamic modulus reached approximately 0.42. Below this point, the short-term sorptivity increased slowly with an increase in the freeze and thaw damage. Above this point, a dramatic increase in the short-term sorptivity was observed as the freeze and thaw damage increased. The presence of the knee point can be explained by two considerations. First, a sudden increase in crack width might occur, leading to a substantial increase in water absorption. It was visually noticed during freeze and thaw testing that the knee point (i.e., E/E_0=0.40) corresponded to a specific deterioration level at which visible cracking occurred. However, previous study indicated that when the relative dynamic modulus approximately reduced to 0.4, the crack width was typically

(a) 60X

(b) 170X

(c) 60X

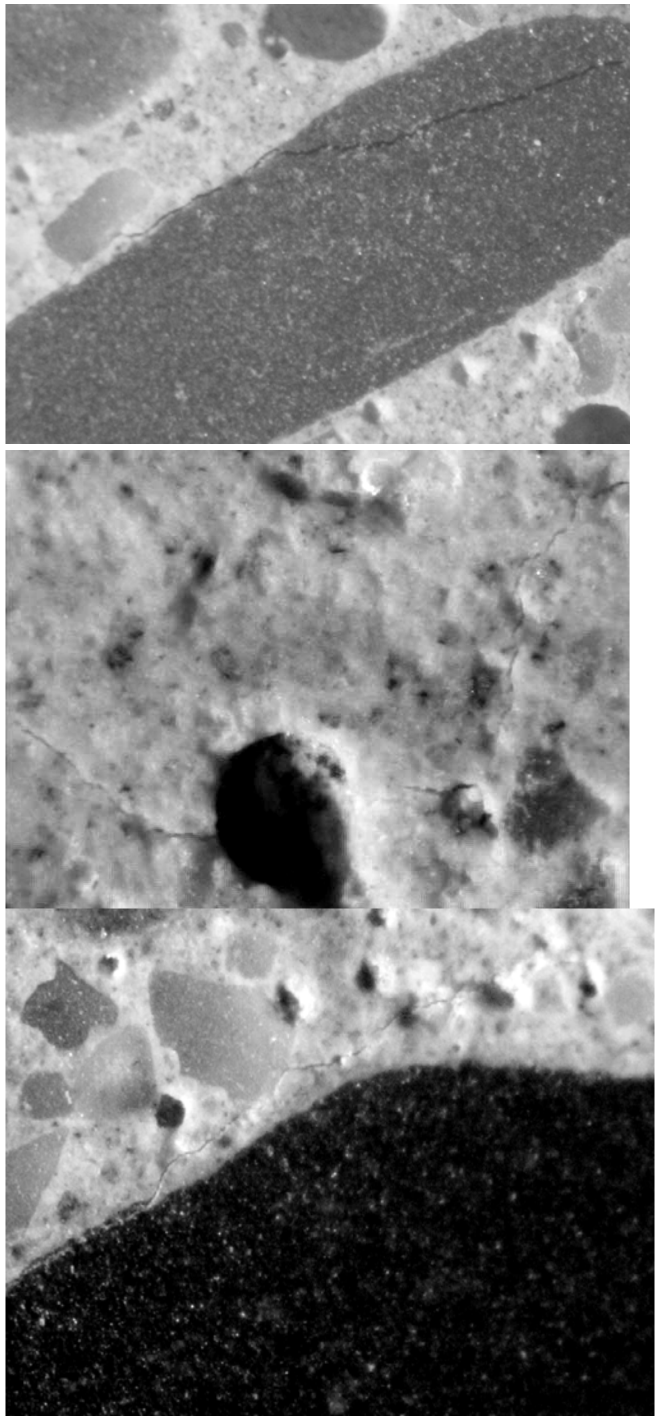

Figure 6. Examples of typical crack patterns, (a) crack through both aggregate and paste (I-70, 6 years), (b) crack through air voids (I-65-T, 25 years), and (c) crack through interface and paste (I-65-U, 25 years)

between 1 μm to 10 μm (Yang et al. 2004). As a result, there would be substantial changes in crack width (from 10 μm to that that is visible to naked eyes) when the relative dynamic modulus approached 0.4. Second, the change in transport mechanisms in cracks may contribute to the formation of knee point. Water transport in unsaturated micro-cracks (e.g., crack width<10 μm) was primarily controlled by capillary effects while the gravitational effects would dominate the water transport in unsaturated visible cracks.

The long-term rate of water absorption (i.e., long-term sorptivity) was determined based on the water absorption between 50 hours and 368 hours while the total absorption simply describes the total volume (or mass) of water that has been absorbed by the concrete after 368 hours of water ponding.. The long-term sorptivity and total absorption can play a key role in determining how long a concrete pavement may take to reach a critical degree of saturation that appears to be related to the onset

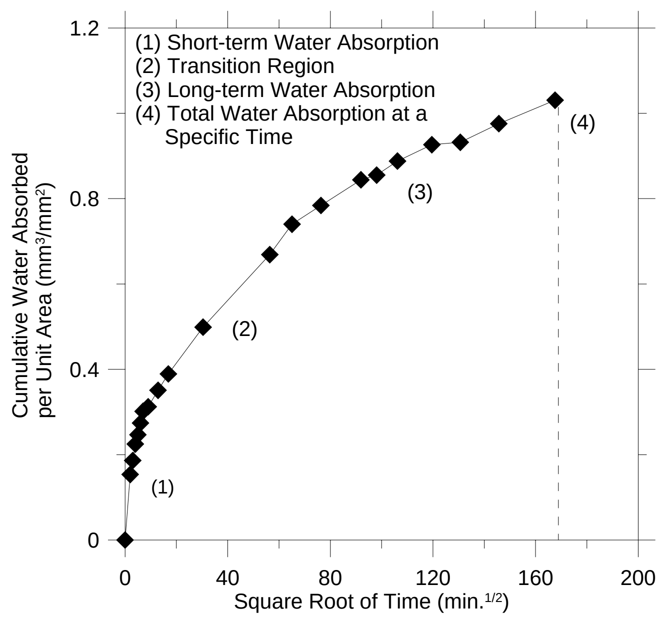

Figure 7. Typical result of water absorption as a function of square root of time

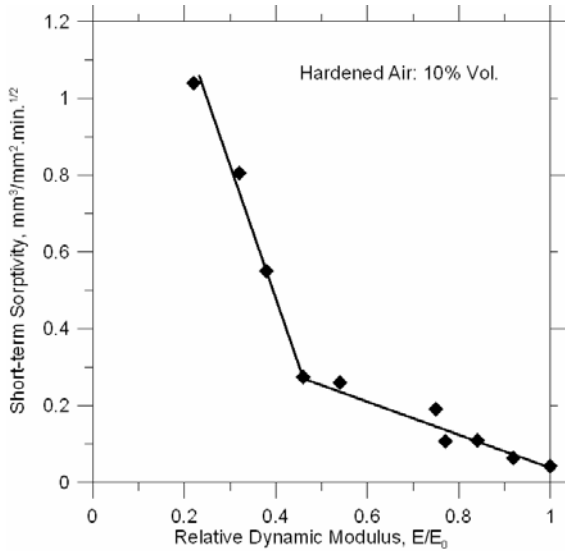

Figure 8. Effects of freeze and thaw damage on short-term sorptivity of concrete

of freeze and thaw deterioration. The long-term sorptivity is commonly thought of as a measure of how quickly and easily the water fills the air voids and large pores (Wilson et al. 1999). It is closely related to characteristic of air void system (e.g., air content and air void size, distribution, spacing, and specific surface area) and degree of damage. Concrete with higher amount of small and well-distributed air voids tends to have higher long-term sorptivity. Cracks may reduce the resistance to diffusion, absorption, and permeation and facilitate the transport of both air and water in concrete. As a result, the presence of cracks in concrete would increase its long-term sorptivity.

Figure 9 shows how freeze and thaw damage and air content influence the long-term sorptivity of concrete using laboratory-cured specimens. It can be seen that concrete that had 10% air content showed higher long-term sorptivity than that which had 6.8% air content. It should be noted that the size, shape, and distribution of the air void system in these specimens (i.e., two air contents) were similar. As a result, concrete that has higher air content would have more air voids and surface areas available for air-water exchange, which would result in higher long-term sorptivity. It can also be seen that the freeze and thaw damage influenced the long-term sorptivity of concrete. When the relative dynamic modulus decreased, the long-term sorptivity was observed to decrease and then to increase. The transition occurred at the point where the relative dynamic modulus was equal to 0.75. Previous study showed that this transition point corresponded to the formation of well-connected crack network (Yang et al. 2004). This can be explained by the fact that cracks influence the rate of pore saturation, the diffusion resistance, and the permeability of concrete. Before the formation of well connected crack network (E/E_0>0.75), long-term water absorption is controlled by both the pore saturation and the gradual filling of air voids. When the freeze and thaw damage increases, the rate of pore saturation would increase due to the fact that cracks facilitate the water movement in concrete. This suggests that the contribution of pore saturation to the long–term water absorption would decrease. As a result, the long-term sorptivity would decrease assuming that isolated cracks do not significantly influence the gradual filling of air voids. After the formation of well connected crack network (E/E_0<0.75), concrete pores can be saturated in much shorter time and the long–term water absorption is primarily dominated by the gradual filling of air voids. When the freeze and thaw damage increases, the air-water exchange would increase due to the fact that cracks may facilitate the diffusion of air and the permeation of water in concrete. As a result, the long-term sorptivity would increase.

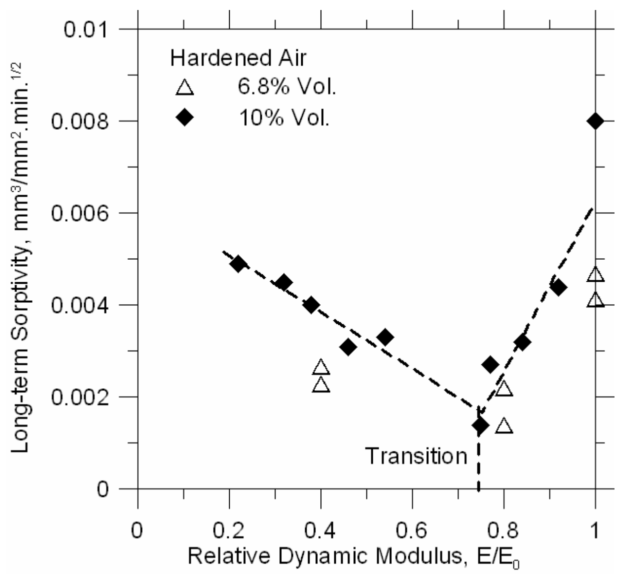

Figure 9. Effects of freeze and thaw damage on long-term sorptivity of concrete

Figure 10 presents the sorptivity results of one pavement section (I-65-T) to illustrate the comparison of sorptivity values that were measured at different locations in the slab. It is clearly seen that cores taken from the joint and edge of the slab behave differently from cores taken from the mid-panel (center) of the slabs. Higher values of sorptivity (including both short-term and long-term) were observed at the middle depth for joints and edges and at the top surface of mid-panel suggesting that more damage may be developing at these locations. The locations close to the joint demonstrate a higher overall sorptivity thereby suggesting that the damage was more uniform at the joints and corners. The reasons for the differences between the behavior of the slab at the center and at the corners may be explained by two considerations. First, at the joint the dowel bars transfer load more uniformly throughout the edge section and may transfer substantial stresses which may result in microcracks due to the restraint of moisture and thermal movements. Second, the joints and edges of the slab are more susceptible to water penetration during rainfall and may be more susceptible to the effects of freezing and thawing.

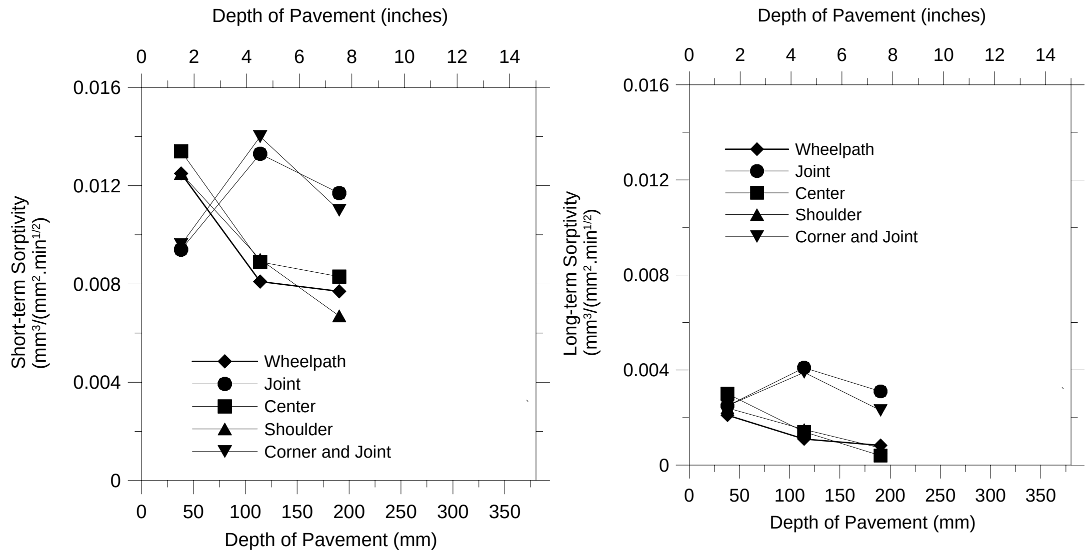

(a) (b)

Figure 10. Changes of sorptivity with locations of the core for one pavement section (I-65-T), (a) Short-term sorptivity, and (b) Long-term sorptivity

Figure 11a shows a comparison of the short-term sorptivity that was obtained by averaging the sorptivty of cores from the center, the wheel path, and the shoulder for pavements from various sections. It can be seen that two sections (I-65-T and I-70) demonstrate a substantially higher short-term sorptivity at the surface than in the middle or bottom of the specimen. This again is consistent with the damage development at the top of the pavement in sections that are showing signs of deterioration (i.e., microcracking was observed under microscopic examination).

An assessment of the influence of traffic loading on the cumulative damage in PCC pavements can be made by comparing the pavement section that was exposed to traffic and the environment (I-65-T) with the section that was only exposed to the environment (I-65-U). In the section exposed to traffic (I-65-T) the short-term sorptivity at the top of the pavement is 54% higher than the short-term sorptivity at the bottom of the core. However, the untrafficed section only showed an increase of short-term sorptivity of 5%. This implies that the combination of traffic loading and environmental attack can accelerate the deterioration since both sections are of the same age and were under essentially the same environment.

In addition, the short-term sorptivity appears to be somewhat related to the age of the specimen. The oldest pavement section (I-65) shows the highest short-term sorptivity, while the short-term sorptivity of new pavement section (I-465) is the lowest. This may be due to an improvement in the mixture proportions/placement procedures over time that has resulted in a tighter, less porous system. In addition to pavement age, damage may also play a part in increasing the short-term sorptivity. For example, although the cores taken from I-70 represent a pavement that is “younger” than the pavement I-469, it has higher sorptivity. This may be explained by the fact that pavement I-70 had started deteriorating based on the microscopic examination, whereas, no cracks were observed in pavement I-469. This is consistent with the results from laboratory-cured specimens (Figure 8) which described that short-term sorptivity of concrete increased with the degree of damage.

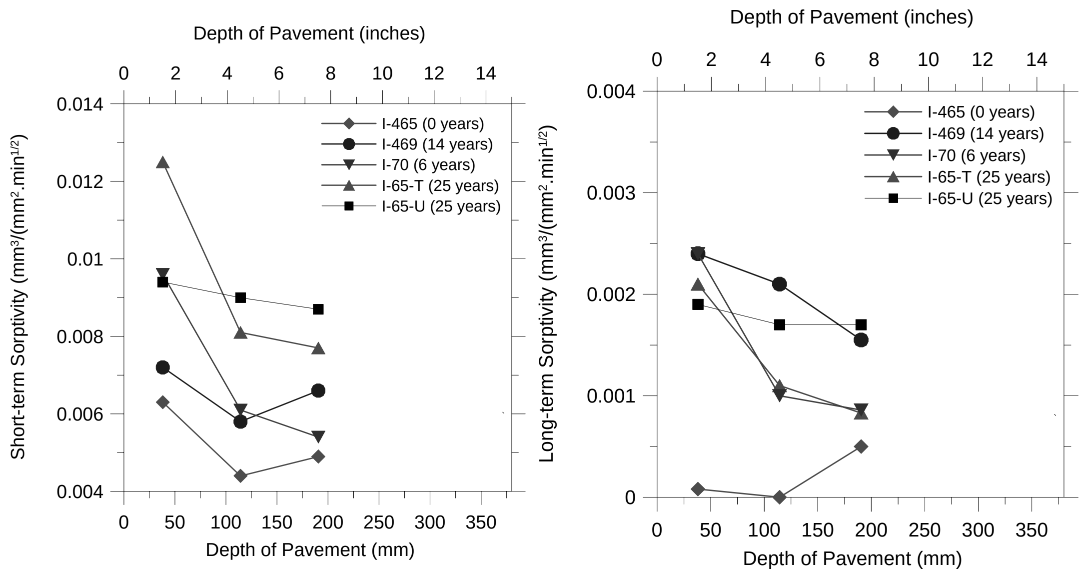

(a) (b)

Figure 11. Change of sorptivity (center, wheel path, and shoulder cores only) with pavement depth for all pavement locations, (a) Short-term sorptivity, and (b) Long-term sorptivity

Figure 11b shows the long-term sorptivity of all pavement sections. Based on the laboratory investigation (as shown in Figure 9), the long-term sorptivity is influenced by the pore structure, air content, and freeze and thaw damage. The interaction between capillary pores, air voids, and damage is complicated due to the fact that the concrete micro-structures and air void systems in these pavements are quite different based on the microscopic examination. Table 3 lists several of the main factors that were measured in these pavements that may be related to the long-term sorptivity. Damage is only identified qualitatively as cracked or uncracked based on microscopic examination. The results in Figure 11b reflect the combined effects of pores, air void system, and damage on the long-term sorptivity. It can be seen from Figure 11b that a good concrete (uncracked I-469) showed higher long-term sorptivity than a cracked concrete (I-70) (Table 3). This agrees well with the results from laboratory-cured specimens (Figure 9), in which a sound concrete (E/E_0=1.0) shows the highest long-term sorptivity. The long-term sorptivity decreased with an increase in the freeze and thaw damage when relative dynamic modulus was above 0.75.

Table 3. Factors That Contribute to Long-Term Sorptivity

Pavement Section	Long Time Sorptivity	Microscopic Investigation of Damage	Air Void System	
			Air Content (%Vol.)	Specific Surface Area * mm^2/mm^3 ($in.^2/in.^3$)
I-65-T	0.001	Cracked	9.6	12.3 (313.1)
I-469	0.0018	Uncracked	7.3	9.5 (240.3)
I-70	0.0009	Cracked	4.6	14.5 (369.4)
I-465	0.00025	Uncracked	11.5	8.3 (209.6)
I-65-U	0.0037	Cracked	9.3	10.2 (258.7)

Splitting Tensile Strength. The split cylinder test was used to provide an indication of the mechanical properties of the concrete pavements. Figure12 shows the splitting tensile strength that was obtained from the cores taken from each of the pavement sections. It can be seen that the splitting tensile strength ranges from 3.1 MPa (450 psi) to 4.3 MPa (630 psi). The new pavement section (I-465) has the highest value, while the I-65-U that is 25 years old shows the lowest value. This may reflect the fact that the variation of splitting tensile strength with depth or pavements can be mainly linked to the age, air voids, and damage of the pavement sections.

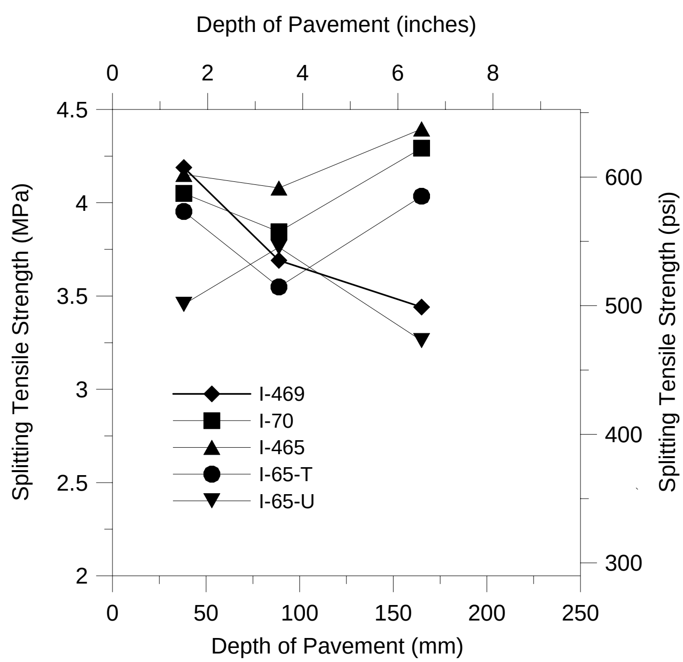

Figure 12. Splitting tensile strength of all pavement sections in this study

Conclusions

This paper has reported the results of field condition assessment of selected concrete pavements in the state of Indiana. Specifically, this work was intended to provide a better understanding of the damage that is present in existing pavements for use in life-cycle modeling. Based on the results obtained from cores taken from several pavements, the following conclusions can be drawn:

- Typical cracks observed in the pavements occur at the aggregate-paste interface, through weak aggregates, and in the paste. While the exact cause of this cracking is not completely known, it is hypothesized that this cracking is due to a combination of loading and environmental effects.
- The average total hardened concrete air contents for these pavements were found to vary widely from approximately 4.0% to 13.0%. Entrapped air may comprise relatively large portions of the total air (from 1.2% to 4.5%). In one pavement relatively large entrapped air voids (up to 25 mm in diameter) were found which could be a result of insufficient closing of the paste after vibration.
- It was observed from laboratory-cured specimens that the short-term sorptivity increases with the freeze and thaw damage in a bilinear fashion while the long-term sorptivity was found to correlate with the freeze and thaw damage and air content. In pavements that are known to be performing poorly (microcracking was observed under microscopic examination) it was observed that the short-term sorptivity near the surface of the pavement was substantially higher (up to 54%) than that in the middle or bottom of the pavement. This indicates that microcracking occurs at the surface of concrete pavements which results in more rapid water transport and absorption. In addition, higher short-term sorptivity was observed in older pavements indicating that damage had been developed and accumulated in these pavements.

Acknowledgements

The work presented herein was conducted as a part of the Joint Transportation Research Program (JTRP) project entitled *Interaction Between Micro-cracking, Cracking and Reduced Durability of Concrete: Developing Methods for Quantifying the Influence of Cumulative Damage in Life-Cycle Modeling.* The authors gratefully acknowledge the support of the Indiana Department of Transportation. The authors also extend their thanks to all the Study Advisory Committee members for their constant advice, and the Research Division, INDOT for their assistance in traffic control and coring.

References

ASTM (1998), "Standard test method for microscopical determination of parameters of the air-void system in hardened concrete," C457-98

ASTM (1996), "Standard test method for splitting tensile strength of cylindrical concrete specimens," C496-96

ASTM (1997), "Standard test method for pulse velocity through concrete," C597-97

ASTM (1999), "Significance of tests and properties of concrete and concrete-making materials," STP 169C

Bentz, D.P., Ehlen, M. A., Ferrais, C. F., and Garboczi, E. J. (2001), "Sorptivity-based service life predictions for concrete pavements," 7th international conference on concrete pavements – Orlando, Florida, USA, Sept. 9-13

Fagerlund, G. (1997a), "Effect of self-desiccation on the internal frost resistance of concrete," *Self-desiccation and its importance on concrete technology*, Persson,B and Fagerlund, G., eds., Lund, Sweden, 227-238.

Fagerlund, G. (1997b), "On the service life of concrete exposed to frost action," *Freeze and thaw durability of concrete*, J. Marchand, M. Pigeon and M. Setzer, eds., E&FN Spon, London, UK, 23-41

Hoerner, T.E. and M. I. Darter (1999), "Guide to developing performance-related specifications for pcc pavements, volume 1: practical guide," Final report and appendix A, FHWA-RD-98-155, Federal Highway Administration, Feb.

Lockington, D., J. Y. Parlange, and P. Dux. (1999), "Sorptivity and the estimation of water penetration into unsaturated concrete," Materials and Structures, 32(6), 342-347

Marchand, J., M. Pigeon, and M. Setzer (1997), "Freeze-thaw durability of concrete," E & FN Spon, London, UK

Martys, N. S., and C. F. Ferraris (1997), "Capillary transport in mortars and concrete," Cement and Concrete Research, 27(5), 747-760

Pavement Management Unit, INDOT (2000), Pavement surface report, December

Popovics, S., J. L. Rose, and J. S. Popovics (1990), "The behavior of ultrasonic pulse in concrete," Cement and Concrete Research, 20, 259-270

Qi, C., W. J. Weiss, and J. Olek (2003), "Quantifying the impact of plastic shrinkage cracking on the corrosion of reinforced concrete to improve service life prediction," ASTM symposia STP 1457, June 18, Denver, CO (in press)

Suaris, W. and V. Fernando (1987), "Ultrasonic pulse attenuation as a measure of damage growth during cyclic loading of concrete," ACI Materials Journal, May-June, 185-193

Van Dam, T. J., N. J. Buch, K. F. Hanson, J. E. Hiller, L. L. Sutter, and R. Muethel (2001), "Michgan's approach to a state-wide investigation of material-related distress (MRD) in concrete pavements," Transportation Research Record, 1775, 1-9

Wang, K., Jansen, D. C. and Shah, S. P. (1997), "Permeability study of cracked concrete," Cement and Concrete Research, 27(3), 381-393

Wiens, U., Meng, B., Schroeder, P., and Schiessl, P. (1997), "Micro-cracking in high-performance concrete- from model to the effect on concrete properties," *Self-desiccation and its importance on concrete technology*, B. Persson and G. Fagerlund, eds., Lund, Sweden, 193-208

Wilson, M.A, M. A. Carter, and W. D. Hoff (1999), "British standard and RILEM absorption tests: a critical evaluation," Materials and Structures, 32, October, 571-578

Yang, Z., "Assessing Cumulative Damage in Concrete and Quantifying Its Influence on Life Cycle Performance Modeling," Ph.D. Dissertation, Purdue University, West Lafayette, IN, August, 2004

Yang, Z., J. Weiss, J. Olek, 2004, "Water Transport in Concrete Damaged by Tensile Loading and Freeze-Thaw Cycling," ASCE Journal of Materials in Civil Engineering, In press.

Yoon, S., K. Wang, W. J. Weiss, and S. P. Shah (2000), "The interaction between loading, corrosion, and serviceability of reinforced concrete," ACI Materials Journal, 97(6), 637-644

Zhou, Y., M. D. Cohen, and W. L. Dolch (1994), "Effect of external loads on the frost-resistant properties of mortar with and without silica fume," ACI Material Journal, 91(6), 595-601